

**Achieving high performance triboelectric nanogenerators
simultaneously with high-voltage and high-charge energy cycle**

Yikui Gao^{a b ‡}, Jiaqi Liu^{c ‡}, Linglin Zhou^{a b *}, Lixia He^{a b}, Di Liu^{a b}, Peiyuan Yang^a,
Bingzhe Jin^{a b}, Zhong Lin Wang^{a b d e f*}, Jie Wang^{a b d*}

^aBeijing Institute of Nanoenergy and Nanosystems, Chinese Academy of Sciences, Beijing 101400, China

^bSchool of Nanoscience and Engineering, University of Chinese Academy of Sciences, Beijing 100049, P. R. China

^cCangzhou Normal University, Cangzhou 061001, P. R. China

^dGuangzhou Institute of Blue Energy, Knowledge City, Huangpu District, Guangzhou 510555, P. R. China

^eGeorgia Institute of Technology, Atlanta, GA 30332, USA

^fYonsei Frontier Lab, Yonsei University, Seoul 03722, Republic of Korea

[‡]These authors contributed equally

*Correspondence:

Email: zhoulinglin@binn.cas.cn, wangjie@binn.cas.cn, zhong.wang@mse.gatech.edu

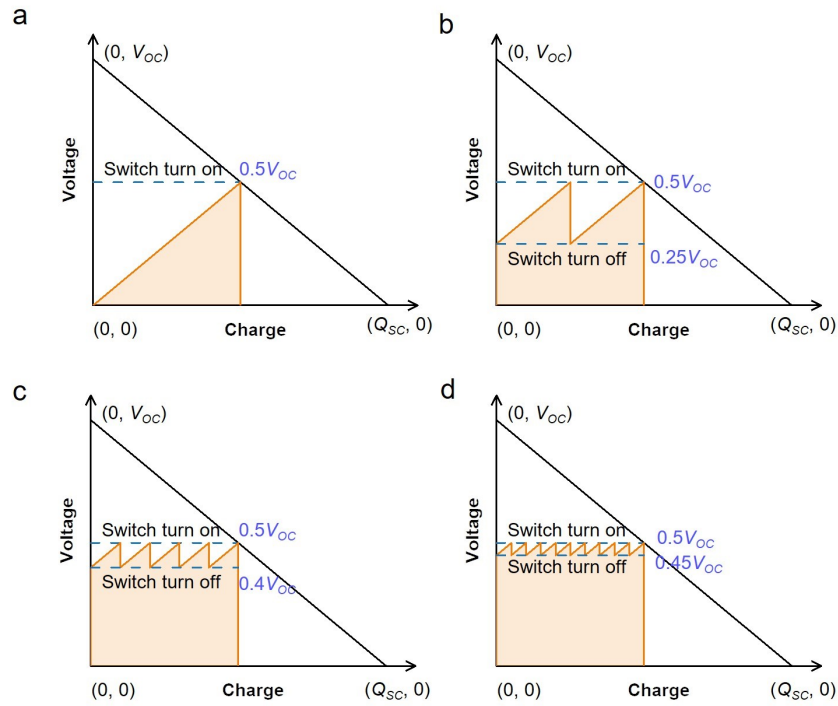


Fig. S1. Cooperating with the switch to achieve 50% energy extraction efficiency.

(a)-(d) When the cut-off voltage of the switch increases from 0 to $0.45 V_{oc}$ respectively, the energy extraction efficiency increases from 25% to 47.5%

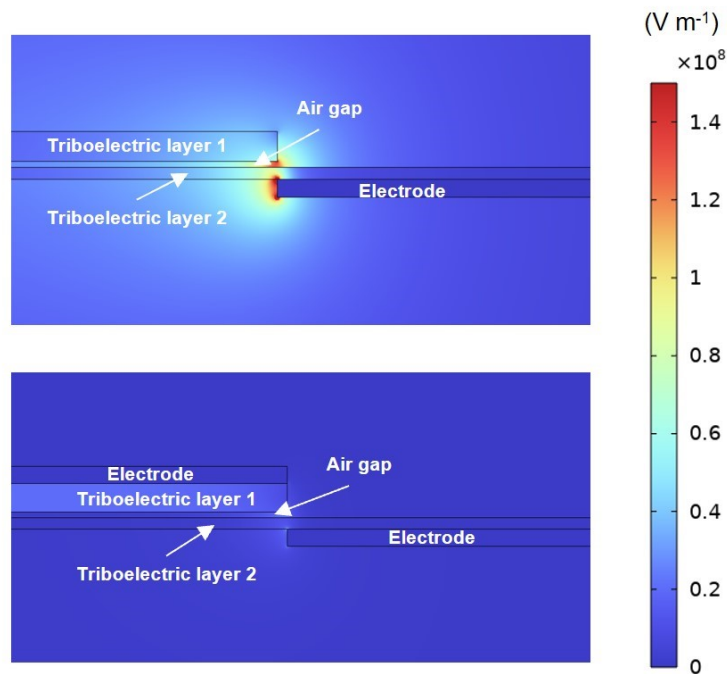


Fig. S2. The simulation results of S-TENG with or without grounded electrode.

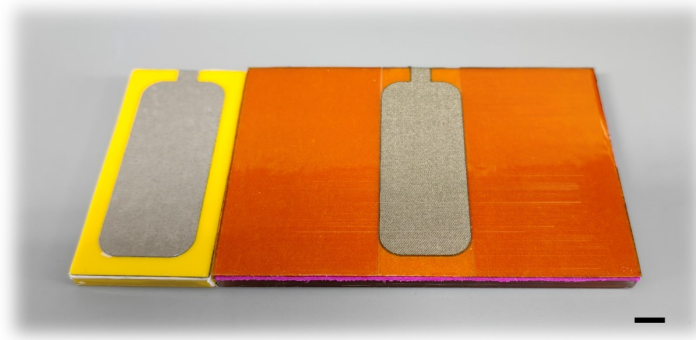


Fig. S3. The photo of S-TENG with PA and PTFE (scale bar: 1 cm).

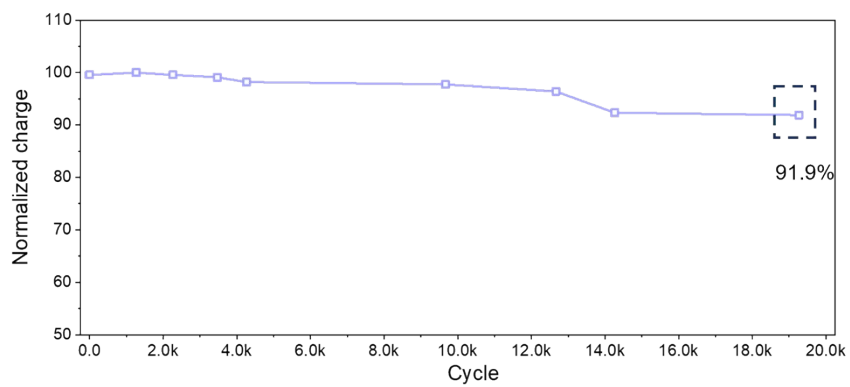


Fig. S4 The stability of S-TENG.

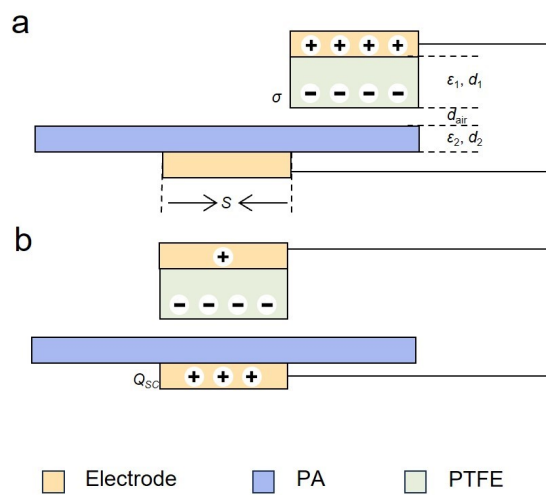


Fig. S5. The relationship between Q_{SC} , d_{air} , d_1 and d_2 .

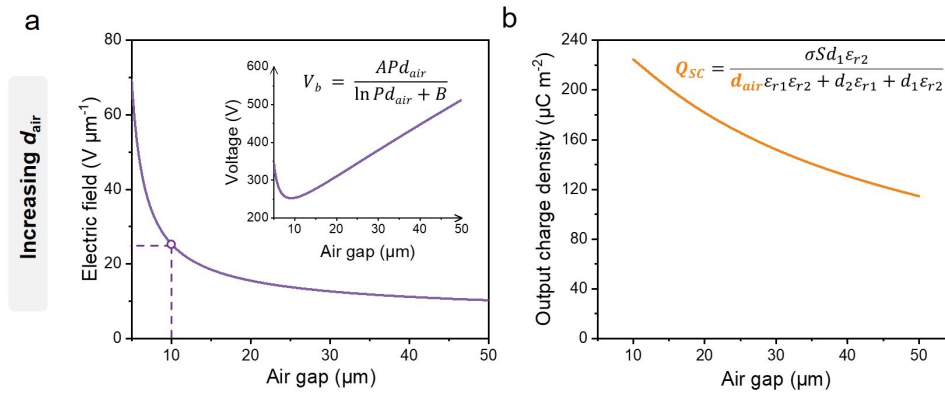


Fig. S6. Increasing the air gap to enhance open-circuit voltage of S-TENG. (a) The threshold electric field of different air gap. (b) The short-circuit charge of S-TENG with the increasing of air gap (assuming surface charge does not decay).

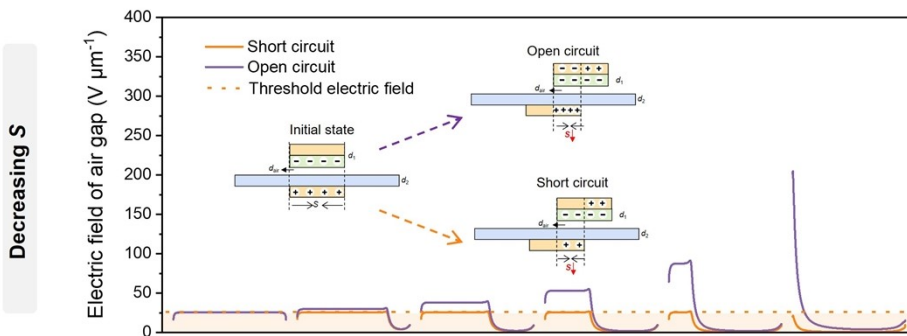


Fig. S7. Decreasing the overlap area of electrodes to enhance open-circuit voltage. Inset figure is the charge distribution when S-TENG is open-circuit state or short-circuit state. The charge density of the electrodes overlap region when S-TENG is open-circuit state is much higher than that when S-TENG is short-circuit state.

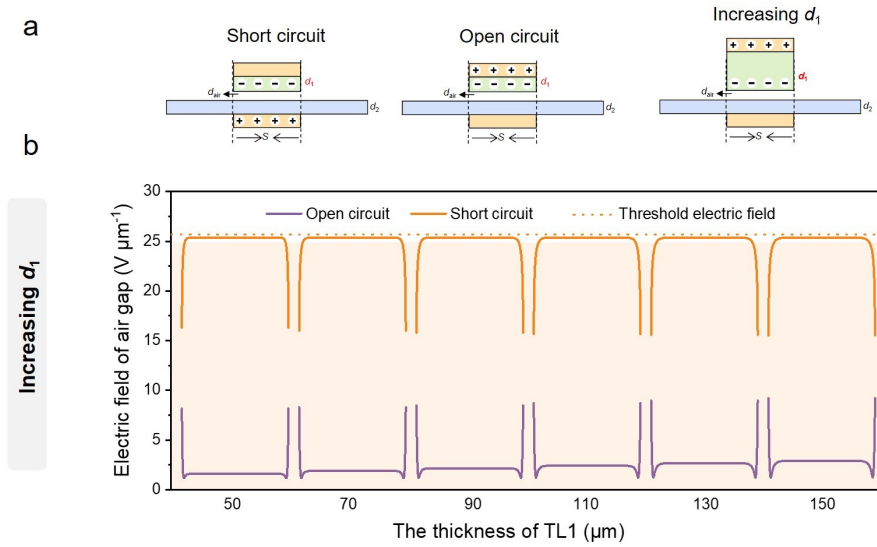


Fig. S8. Increasing the thickness of TL1 to enhance open-circuit voltage. (a) The charge distribution of S-TENG. compared to the charge distribution in short-circuit state, the induced charge of top electrode can weak the electric field of air gap in open-circuit state. (b) The electric field at air gap of S-TENG.

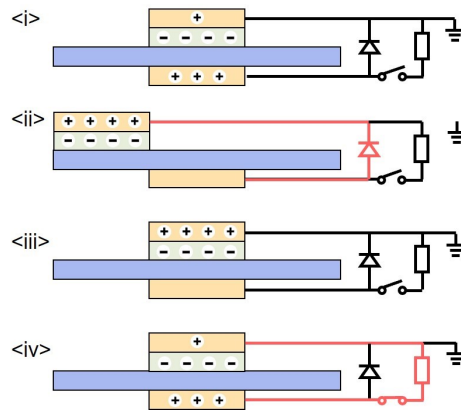


Fig. S9. The working mechanism of S-TENG with mechanical switch.

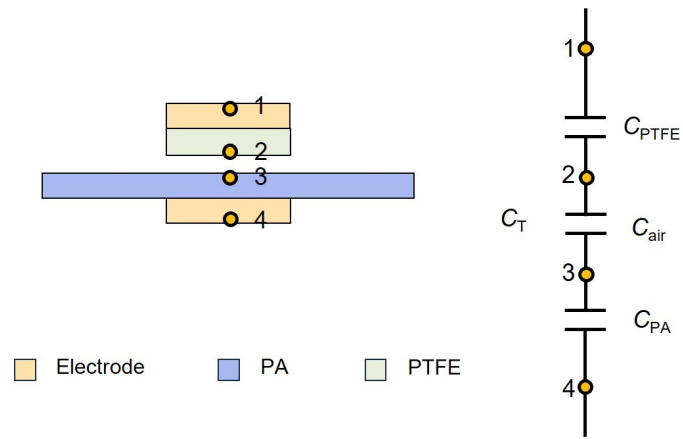


Fig. S10. The equivalent capacitance model of S-TENG.

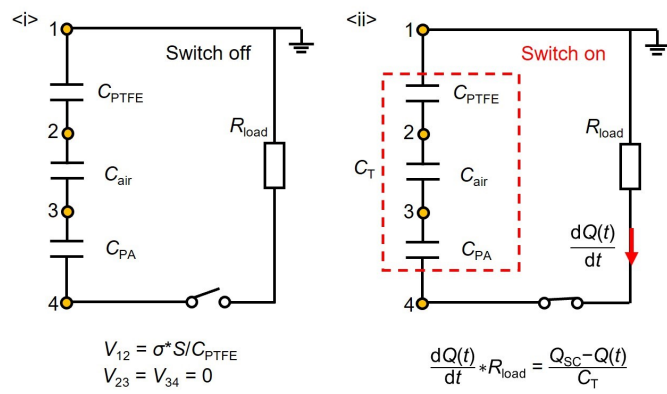


Fig. S11. The equivalent circuit diagram of S-TENG.

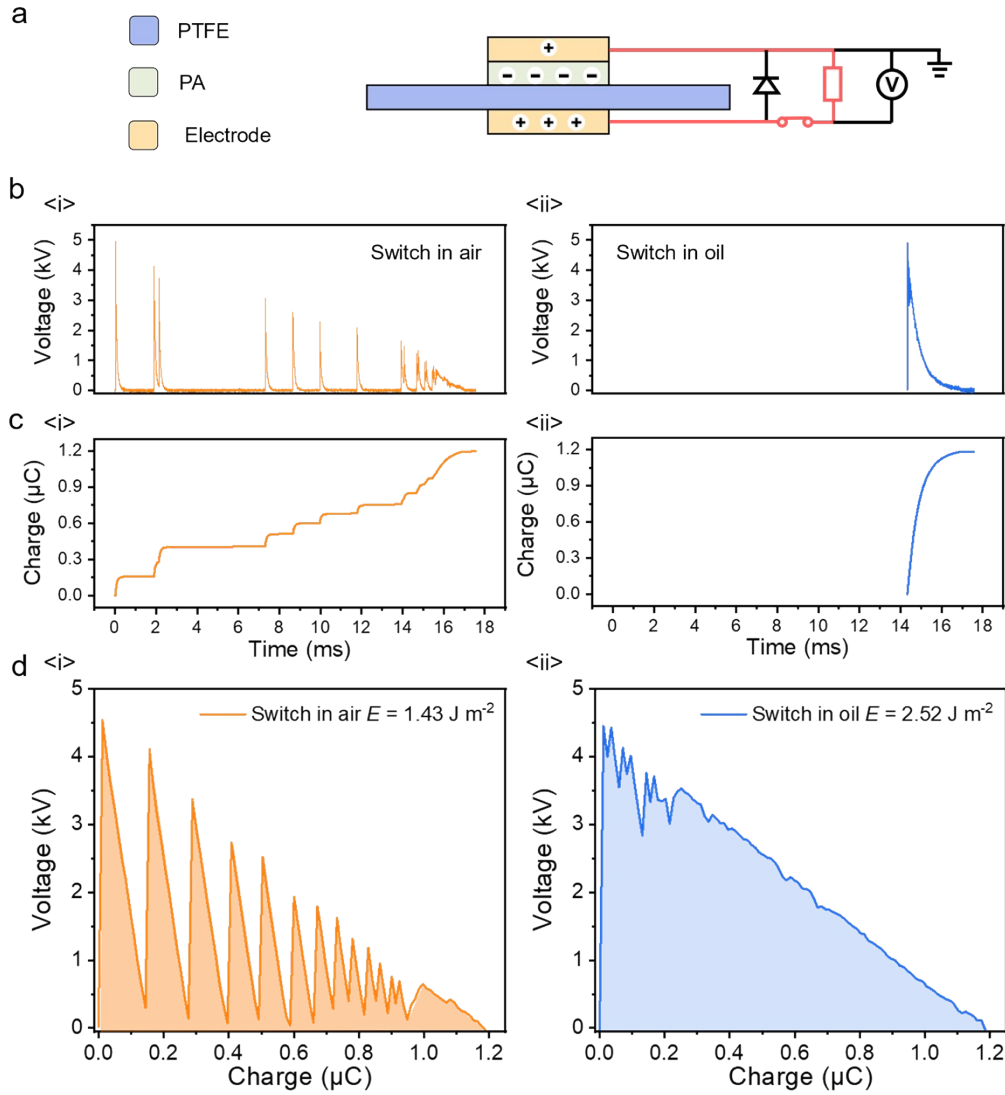


Fig. S12. The test method for HV-HQ energy cycle. (a) The test circuit diagram. (b) The output voltage of S-TENG when the synchronous switch in <i> air and <ii> oil. (c) The output charge of S-TENG when the synchronous switch in <i> air and <ii> oil. (d) The energy cycle of S-TENG when the synchronous switch in <i> air and <ii> oil.

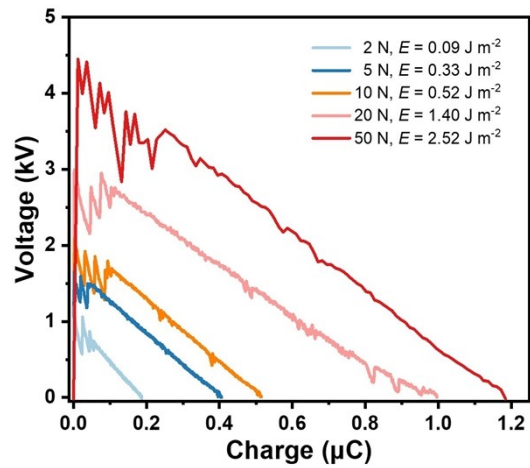


Fig. S13. The energy cycle of S-TENG with different pressure (changing the surface charge density of S-TENG by changing pressure).

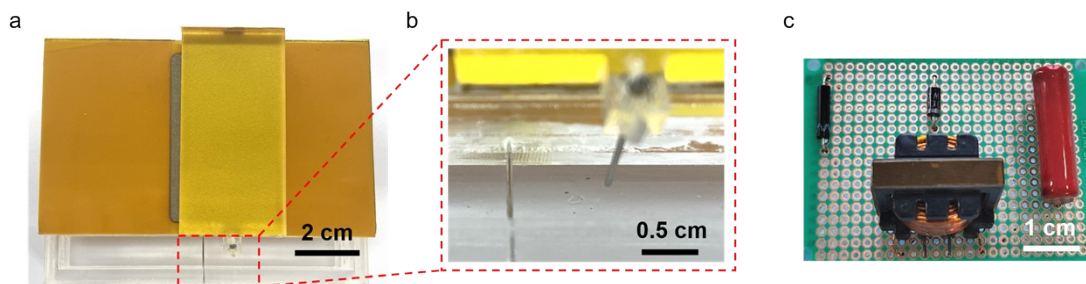


Fig. S14 The photos of (a) S-TENG, (b) synchronous switch and (c) PMC.

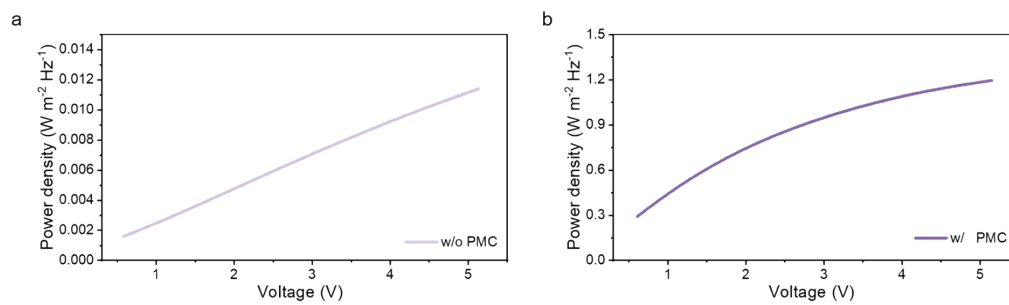


Fig. S15. The output power of S-TENG (a) without PMC and (b) with PMC in the low-voltage range of 0-5 V.

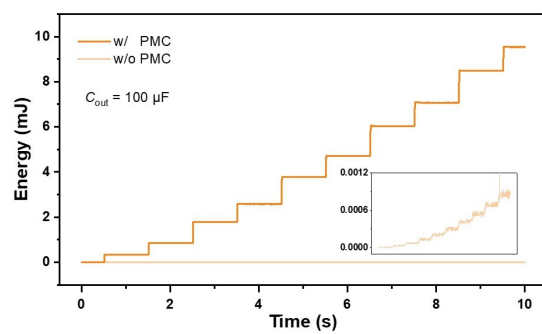


Fig. S16. The output energy of S-TENG with/without PMC.

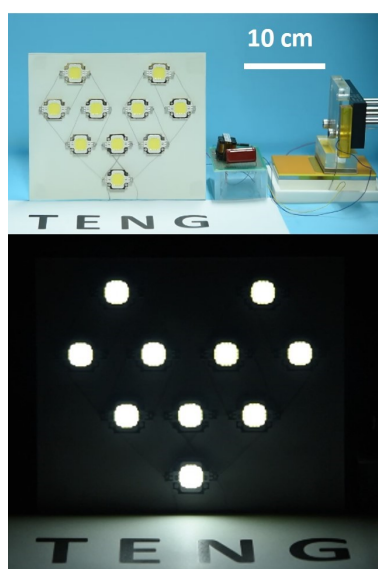


Fig. S17. The S-TENG powered ten bulb lamps with PMC.

Supplementary Table 1 The parameters of finite element simulated calculation for Fig. 2c and Fig. 3e

The thickness of TL1	50 μm
The thickness of TL2	20 μm
The relative dielectric constant of TL1	2
The relative dielectric constant of TL2	3
The surface charge density of TL1	374 $\mu\text{C m}^{-2}$
Air gap	10 μm

Supplementary Table 2 The parameters of finite element simulated calculation for Fig. 3e

The thickness of TL1	30/50/70/90/110/130/150 μm
The thickness of TL2	20 μm
The relative dielectric constant of TL1	2
The relative dielectric constant of TL2	3
The surface charge density of TL1	473/374/331/307/292/282/274 $\mu\text{C m}^{-2}$
Air gap	10 μm

Supplementary Note 1 Optimal input capacitor and input voltage

As the charge stored in C_{in} gradually increases, its voltage also increases ($V = Q/C$). When the V - Q curve of C_{in} intersects with CMEQ of TENG, the voltage of C_{in} will no longer increase (At this point, the voltage of C_{in} is equal to the output voltage of TENG) and the area enclosed by the V - Q curve of C_{in} is the energy extracted by C_{in} from TENG (Fig. 1b <i>, the shaded area represents the energy stored by C_{in} >). Therefore, the energy of C_{in} can be calculated as:

$$E = \frac{C_{in}Q_{SC}^2}{2(C_{in} + C_T)^2} \quad (1)$$

C_T is the inherent capacitor of TENG. Only when C_{in} is equal to C_T , the maximum energy can be obtained:

$$E_{max} = 0.125 * Q_{SC}V_{OC} \quad (2)$$

Obviously, just 25% of TENG's maximum energy output can be obtained by this strategy.

On the other hand, maintaining a fixed voltage of C_{in} , and then extracting energy from TENG is an interesting strategy to obtain more energy. As shown in Fig. 1b <ii>, when the voltage of C_{in} is fixed, the area enclosed by the V - Q curve changes from a triangle to a rectangle and the energy can be calculated as:

$$E = V_{in}(Q_{SC} - V_{in}C_T) \quad (3)$$

where V_{in} is the voltage of C_{in} , and only when V_{in} is equal to $0.5*V_{OC}$, the maximum energy can be obtained.

$$E_{max} = 0.25 * Q_{SC}V_{OC} \quad (4)$$

Therefore, the energy extraction efficiency can be improved to 50%.

In fact, parasitic capacitor (C_p) is inevitable in the process of device manufacturing and circuit design. This means that C_T in the formula (1)-(4) must be replaced with (C_T+C_p) . However, due to the uncertainty of C_p , it is difficult for us to accurately calculate the optimal C_{in} and V_{in} . Therefore, in actual circuit design, they still need to be determined through experimental iteration.

Supplementary Note 2 Cooperating with the switch to achieve 50% energy extraction efficiency

For the conventional step-down circuit, the role of switch is to adjust the duty ratio to regulate output voltage. However, for TENG's step-down circuit, the other role of switch is to release the energy stored in C_{in} to obtain high peak current and achieve high efficiency of circuit^{1,2}. Because the intrinsic low output current of TENG will lead to extremely low energy utilization if utilized directly.

Generally, when the switch turns on, the energy stored in C_{in} will be released to 0 in a few hundred microseconds (the time is related to the product of C_{in} and inductance), and then the voltage of C_{in} also decreases to 0. Therefore, just 25% of TENG's maximum energy output can be utilized (Fig. S1a). Interestingly, if the voltage of does not decrease from $0.5 V_{oc}$ to 0, but instead to $0.25 V_{oc}$, $0.4 V_{oc}$ or $0.45 V_{oc}$, the energy extraction efficiency will be increased to 37.5%, 45%, 47.5% respectively (Fig. S1b-d). The closer the cut-off voltage of the switch is to $0.5 V_{oc}$, the higher the energy obtained.

Supplementary Note 3 The method for 50% energy extraction efficiency

To achieve the condition stated in Fig. 1b <ii>, the coordination of synchronous switches is necessary. Here, we assume that the conduction time of the synchronous switch is T_{on} , and the time required for the input capacitor (C_{in}) to release energy to the inductor (L) is T_1 . Only when T_1 exceeds T_{on} will the residual voltage of C_{in} after each cycle not drop to 0, thereby achieving the condition stated in this paper. Therefore, reducing T_{on} of the synchronous switch or increasing T_1 are both feasible strategies. According to the working principle of the LC step-down circuit, T_1 can be calculated as:

$$T_1 = \frac{\pi}{2} \sqrt{\frac{LC_{in}C_{out}}{C_{in} + C_{out}}} \quad (5)$$

Where C_{out} is the output capacitor. Generally, C_{out} is significantly greater than C_{in} , thus T_1 also can be regarded as:

$$T_1 \approx \frac{\pi}{2} \sqrt{LC_{in}} \quad (6)$$

Therefore, we can increase T_1 by increasing C_{in} or L .

Supplementary Note 4 The relationship between Q_{SC} , d_{air} , d_1 and d_2

Although the inherent capacitor (C_T) can be decreased by decreasing d_{air} and d_2 , which also cause a decrease of Q_{SC} . The detail analyses are as follows:

Here, we assume that the surface charge density of polytetrafluoroethylene (PTFE) is σ , the area of electrode is S , the thickness of PTFE and nylon (PA) is d_1 and d_2 , the relative dielectric constant of PTFE and PA is ε_1 and ε_2 , the air gap is d_{air} . The relative dielectric constant of air is 1, and the vacuum dielectric constant (ε_0) is 8.854×10^{-12} .

According to Gauss's theorem (ignoring edge effect), the electric field across the air gap (E_{air}) of **Fig. S5b** can be described as:

$$E_{air} = \frac{Q_{SC}}{S\varepsilon_0} \quad (7)$$

The electric field across the PTFE (E_{d1}) is:

$$E_{d1} = \frac{\sigma S - Q_{SC}}{S\varepsilon_0\varepsilon_1} \quad (8)$$

The electric field across the PA (E_{d2}) is:

$$E_{d2} = \frac{Q_{SC}}{S\varepsilon_0\varepsilon_2} \quad (9)$$

Therefore, the potential difference between two electrodes (V_{12}) is:

$$V_{12} = E_{air}d_{air} + E_{d1}d_1 + E_{d2}d_2 \quad (10)$$

V_{12} is zero, as S-TENG is short-circuit state. Combining equation (7)-(10), the relationship between Q_{SC} , d_{air} , d_1 and d_2 is:

$$Q_{SC} = \frac{\sigma S d_1 \varepsilon_2}{d_{air} \varepsilon_1 \varepsilon_2 + d_2 \varepsilon_1 + d_1 \varepsilon_2} \quad (11)$$

According to formula (9), the increase of d_2 or d_{air} will cause the decrease of Q_{SC} .

Supplementary Note 5 Dielectric breakdown in S-TENG

Currently, air breakdown is a key factor to limit the performance improvement of TENGs. Although this work utilizes a half-wave circuit to avoid air breakdown caused by high output voltage, dielectric breakdown remains a challenge that must be addressed to further enhance charge density. In our previous study³, we reported that the critical breakdown field strength of Polytetrafluoroethylene (PTFE) is about $110 \text{ V } \mu\text{m}^{-1}$. This means that dielectric breakdown is only possible when the surface charge density of PTFE reaches 2.4 mC m^{-2} according to the formular (12).

$$E_B = \frac{\sigma_B}{\varepsilon_0 \varepsilon_1} \quad (12)$$

Where E_B is the critical breakdown field strength of dielectric, σ_B is the surface charge density of dielectric, ε_0 is the vacuum permittivity, ε_1 is the relative permittivity of dielectric (the relative permittivity of PTFE is about 2.5.). There is only $1.1\sim 1.2 \text{ mC m}^{-2}$ in this work, so this process does not cause any damage to the electrodes or dielectric films.

Supplementary Note 6 The critical electric field value of S-TENG

The maximum output charge density (σ_{\max}) of TENGs is defined as the output charge in short-circuit state⁴, which is affected by three factors: the triboelectrification charge density ($\sigma_{\text{triboelectrification}}$), the remaining surface charge density after the air breakdown between two triboelectric layers ($\sigma_{\text{air breakdown}}$), and the maximum charge density that the dielectric can store ($\sigma_{\text{dielectric breakdown}}$).

$$\sigma_{\max} = \min(\sigma_{\text{triboelectrification}}, \sigma_{\text{air breakdown}}, \sigma_{\text{dielectric breakdown}}) \quad (13)$$

The charge density of TENGs can be increased with the enhancement of $\sigma_{\text{triboelectrification}}$ by materials optimization and structure design. However, with rising charge density on dielectric surface, the air breakdown will occur between two triboelectric layers and part of charges will be released, resulting in the limitation of $\sigma_{\text{air breakdown}}$. $\sigma_{\text{dielectric breakdown}}$ is always larger than $\sigma_{\text{air breakdown}}$ in air atmosphere, because the breakdown threshold of air is lower than that of dielectric.

For S-TENG fabricated by PTFE and PA, $\sigma_{\text{triboelectrification}}$ generally is larger than $\sigma_{\text{air breakdown}}$, due to the high efficiency of sliding triboelectrification. Therefore, air breakdown is an important factor limiting S-TENG's performance improvement. In other word, when the output charge of S-TENG in short-circuit state reaches the maximum value, the electric field intensity of air gap can be considered as the threshold for air breakdown.

As shown in Fig. 3e, with the decrease of S , the electric field increase rapidly and exceed that of short-circuit state. However, benefitting by the electrostatic shielding effect of back electrode Fig. 3f, the electric field with the increase of d_1 is always below that of short-circuit state.

Supplementary Note 7 The solution of the circuit's the dynamic equation

The equivalent circuit diagram of S-TENG is shown in Fig. 4b. The initial state of circuit is as follows:

$$V_{12} = \sigma^*S/C_{\text{PTFE}} \quad (14)$$

$$V_{23} = V_{34} = 0 \quad (15)$$

According to Kirchhoff's voltage law, when the switch turns on, the circuit's the dynamic equation is:

$$\frac{\sigma S - Q(t)}{C_{\text{PTFE}}} - \frac{dQ(t)}{dt}R_{\text{load}} - \frac{Q(t)}{C_{\text{air}}} - \frac{Q(t)}{C_{\text{PA}}} = 0 \quad (16)$$

Where $Q(t)$ is the amount of charge transferred in the circuit. According to formula (9),

$$\frac{\sigma S}{C_{\text{PTFE}}} = \frac{Q_{\text{SC}}}{C_{\text{T}}} \quad (17)$$

Therefore, formula (13) can be showed as:

$$\frac{Q_{\text{SC}} - Q(t)}{C_{\text{T}}} - \frac{dQ(t)}{dt}R_{\text{load}} = 0 \quad (18)$$

Formula (18) is the dynamic equation of circuit that shown in Fig. S11, therefore the energy that can be utilized during this process (Fig. 4a) is equivalent to the energy stored in C_{T} with an initial charge of Q_{SC} .

Supplementary Note 8 The test method for HV-HQ energy cycle

The test circuit for the energy cycle is shown in Fig. S12a. Using a mixed domain oscilloscope (MDO3024) as the voltmeter, and its probe model employed is the Tektronix P6015A, which has an internal resistance of 100 M Ω and a voltage range of 20 kV. To ensure the accuracy of the test results, the circuit's test resistance should be significantly lower than the probe's internal resistance (in this study, the test resistance is set to 2 M Ω). The working mechanism of the S-TENG with a synchronous switch is illustrated in Fig. 4a. Clearly, before the synchronous switch is closed, the voltage across the test resistance is zero. When the synchronous switch is closed, the voltage across the test resistance is depicted in Fig. S12b. Consequently, the output charge can be calculated as follows:

$$Q = \int \frac{V}{R} dt \quad (19)$$

The calculated result shown in Fig. S12c. The energy cycle curve can be obtained by taking charge as the horizontal axis and voltage as the vertical axis (Fig. S12d).

Supplementary Note 9 The performance of TENG PMC in the low-voltage range

TENG can effectively convert ubiquitous mechanical motions into electricity, bringing an innovative energy harvesting and conversion technology to the new era of the Internet of Things (IoTs). It is noteworthy that most sensor components, including wearable devices, and energy storage devices, operate at voltages below 5V. The ultimate goal of TENG is to serve as a portable power source for these electronic devices. Therefore, comparing the power output within this voltage range is more aligned with TENG's application requirements.

Due to the high internal resistance characteristics of TENG, the output power of TENG increases linearly with the increasing of output voltage at low output voltage. However, the output power of TENG in the low-voltage range of 0-5 V is much lower than its maximum output power (Fig. S15a).

The purpose of the power management circuit (PMC) is to convert all of TENG's electrical output energy into usable electrical energy for powering electronic devices directly. This ensures that the output power should remain relatively stable across different output voltages. However, due to the voltage drop of the freewheeling diode, when the output voltage is low, there is significant energy loss on the freewheeling diode, resulting in a relatively low power output⁵. As the output voltage increases, the impact of the diode's voltage drop on power gradually decreases, leading to an increase in power output and eventually stabilizing (Fig. S15b).

In summary, it is precisely because of the different growth trends of power output in these two situations that the rate of power increment gradually decreases as the output voltage increases.

Supplemental References

1. Wang, Q. Tang, C. Shan, Y. Du, W. He, S. Fu, G. Li, A. Liu, W. Liu and C. Hu, *Energy & Environmental Science*, 2021, **14**, 6627-6637.
2. Z. Wang, W. Liu, W. He, H. Guo, L. Long, Y. Xi, X. Wang, A. Liu and C. Hu, *Joule*, 2021, **5**, 441-455.
3. J. Zhang, D. Liu, J. Shi, P. Yang, S. Li, Z. Zhao, Z. Guo, Y. Gao, L. He, J.-S. Zhao, J. Wang and Z. L. Wang, *Nano Energy*, 2024, **124**, 109517.
4. J. Wang, C. Wu, Y. Dai, Z. Zhao, A. Wang, T. Zhang and Z. L. Wang, *Nature Communications*, 2017, **8**, 88.
5. Z. Zhang, G. Gu, W. Zhang, G. Gu, W. Shang, Y. Liu, G. Cheng and Z. Du, *Nano Energy*, 2023, 110, 108360.